Preprints (www.preprints.org) | NOT PEER-REVIEWED | Posted: 4 October 2021 doi:10.20944/preprints202110.0053.v1

Article

Synthesis method and thermodynamic characteristics of anode material Li_3FeN_2 for application in lithium-ion batteries

Anatoliy Popovich [1], Pavel Novikov [1], Qingsheng Wang [2], Konstantin Pushnitsa [1], and Daniil Aleksandrov [1,*]

[1] Peter the Great St. Petersburg Polytechnic university, Saint Petersburg, Russia; director@immet.spbstu.ru;
[2] CHN/RUS New Energy and Material Technology Research Institute, Changxing, China; envbattery@yandex.ru;
* Correspondence: aleksandrov_ds@spbstu.ru

Abstract: Li_3FeN_2 material was synthesized by two-step solid-state method from Li_3N (adiabatic camera) and FeN_2 (tube furnace) powders. Phase investigation of Li_3N, FeN_2 and Li_3FeN_2 were carried out. Discharge capacity of Li_3FeN_2 is 343 mAh g^{-1}, that is about 44.7% of theoretic capacity. The molar heat capacity of Li_3FeN_2 at constant pressure in the temperature range 298-900 K should be calculated as $C_{p,m} = 77{,}831 + 0{,}130 \times T - 6{,}289 \times T^{-2}$, where T is absolute temperature, . Thermodynamic characteristics of Li_3FeN_2 were determined as next: entropy S^0_{298} = 116.2 J mol^{-1} K^{-1}, molar enthalpy of dissolution $\Delta_d H_{LFN}$ = - 206,537 ± 2,8 kJ mol^{-1}, the standard enthalpy of formation $\Delta_f H^0$ = - 291.331 ± 5.7 kJ mol^{-1}, entropy S^0_{298} = 113.2 J mol^{-1} K^{-1} (Neumann-Kopp rule) and 116.2 J mol^{-1} K^{-1} (W.Herz rule), the standard Gibbs free energy of formation $\Delta_f G^0_{298}$ = -276,7 kJ mol^{-1}.

Keywords: lithium-ion battery; anode battery; lithium-ion thermodynamics; solid-state synthesis

1. Introduction

Increasing energy needs in modern society, the concern over the fossil energy crisis and the demand for environmental sustainability leads to the search for any possible energy resources, such as renewable energy.

Electrochemical energy storage methods play an increasingly important role in transport and stationary applications. The lithium ion battery (LIB) is one of the best decisions in the field of electrochemical energy storage as a technology and market of choice for portable electronics, backup power and vehicle electrification. To meet high standard requirements, such as high energy density, high power density, long service life, low cost, environmental friendliness and safety, a lot of effort was directed to the development of more advanced batteries, i.e. the attempt on nanostructural material for electrode materials [1-2], increasing the capacity and voltage of cathode materials [3], safety issues [4]. As a promising source of energy for the electric car revolution, LIB has proven its market position. There are a lot of anode materials that attracted attention due to their high theoretical specific capacities [5, 6].

Previous works shows good electrochemical properties of Li_3N-type anodes, e.g. $Li_2Na_4N_2$ and $Li_4Na_2N_2$ phases [7], LiBeN [8], Li_3N-Mg_3N_2 [9] and others.

Li_3FeN_2 first was obtained by Frankenburger et al. by reaction of lithium nitride (Li_3N) with elemental iron in nitrogen atmosphere [10]. After decades, Fromont investigated the reaction of Li_3N with iron using thermogravimetry [11]. These studies shows that Li_3FeN_2 was indexed by an orthorhombic cell with lattice parameters a = 9.65 Å, b = 8.66 Å and c = 8.38 Å.

In this article two-step synthesis and properties of promising anode material Li_3FeN_2 is shown. Firstly, Li_3N synthesis was obtained at adiabatic chamber. Then, mixed with iron nanopowder, Li_3FeN_2 was obtained at tube furnace.

Preprints (www.preprints.org) | NOT PEER-REVIEWED | Posted: 4 October 2021 doi:10.20944/preprints202110.0053.v1

2. Materials and Methods

A 16 mm diameter and 0.6 mm lithium plate sliced and polished in argon glovebox, iron nanopowder, nitrogen and ammonia (NH_3) were used as starting components for Li_3N, Fe_2N and Li_3FeN_2 synthesis (Table 1). Lithium sliced plates were put into titanic autoclave nitrogen filled bomb of Netzsch APTAC 264 as shown on Figure 1. The Li_3N synthesis parameters are next: temperature is 170°C, heat rate 2°C/min, synthesis time 6h and nitrogen pressure is ~709.3 kPa (7 atm).

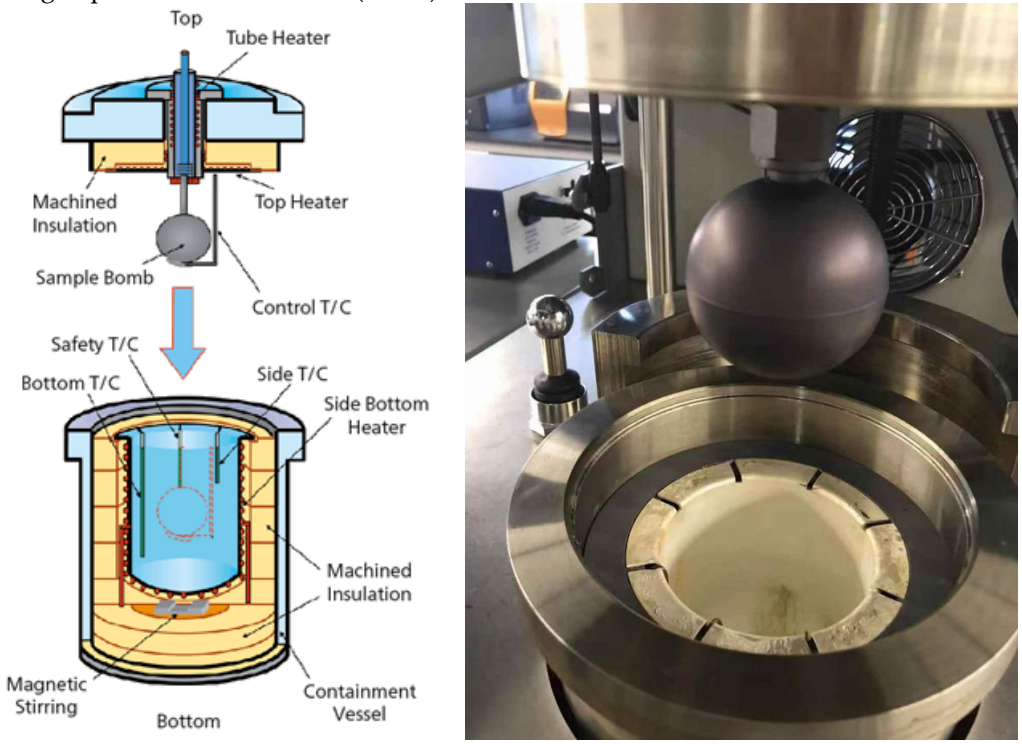

(**a**) (**b**)

Figure 1. Scheme (a) and photo (b) of Netzsch APTAC chamber. 1-machined insulation; 2-sample bomb; 3-safety thermocouple; 4-bottom thermocouple; 5-magnetic stirring; 6-containment vessel; 7-machined insulation; 8-side bottom heater; 9-side thermocouple; 10-control thermocouple; 11-top heater; 12-tube heater.

Iron nanopowder and nitrogen were used as source for Fe_2N. Ceramic crucible with initial powder was put into tube furnace (BTF-1700C). Tube was purged by ammonia (NH_3) for 30 min before synthesis. Synthesis was carried out in NH_3 atmosphere at 530°C for 6h with heat rate of 8°C/min. Mechanically mixed and powder was hot pressed for 2 hours at 1100°C. Received hot pressed sample was heated at N_2 atmosphere for 10 h at 700°C (heat rate was 5°C/min). After heat treatment, sample was mechanically grinded into ivory colored powder.

XRD analysis was held with Bruker D8 Advance with a step of 0.02°. Structural parameters were refined by the Rietveld method using TOPAS5 software.

Preprints (www.preprints.org) | NOT PEER-REVIEWED | Posted: 4 October 2021 doi:10.20944/preprints202110.0053.v1

Table 1. Summary of chemicals descriptions.

Name	Formula	Source	Purity, %
Iron nanopowder	Fe	Changsha Easchem Co., Ltd.	99.9
Lithium	Li	Xiamen Tmax Battery Equipments Ltd.	99.9
Nitrogen	N2	Qingdao Guida Special Gas Co., Ltd.	99.9-99.999
Ammonia	NH_3	Wuhan Newradar Trade Company Ltd.	99.9
Lithium nitride	Li_3N	prepared here	98.9 [1]
Iron nitride	Fe_2N	prepared here	98.4 [1]
Lithium iron nitride	Li_3FeN_2	prepared here	99.1 [1]

[1] Purity according to XRD analysis

Lithium plate, the same as described above, was used as a counter-electrode. 25 μm thickness Celgard 2400 was used as separator. Electrolyte solution was 1.1 M $LiPF_6$ in diethyl carbonate: dimethyl carbonate: ethylene carbonate (DEC/DMC/EC) 1:1:1 by mass mixture. Mixture of 80% Li_3FeN_2 powder, 10% of conductive additive (Super P) and 10% of polyvinylidene fluoride, dissolved in N-methylpyrrolidon was used as experimental electrode.

The synthesized nitrides powders were examined by X-ray diffraction analysis (XRD). XRD was performed with Bruker D8 ADVANCE diffractometer with a vertical goniometer and Cu K_α-radiation. Diffraction angles (2θ) are 5-100º, 10-80º and 5-120º for Li_3N, Fe_2N and Li_3FeN_2, respectively.

Electrochemical tests were performed with battery test system BTS NEWARE CT-3008-5V10 mA (NEWARE, China).

Calorimetric measurements were performed using TAM IV Microcalorimeter at 298 K with the cell volume of 20 ml. Calorimetric cell was filled with aqueous solution of 1 mol dm^{-3} HCl (~ 5 ml) and the ampoule was placed inside the cell in a special holder. The ampoule was broken when thermal equilibrium was established, and nitride powder began to dissolve in HCl solution. Thermo-EMF vs. time was registered during the dissolution process providing the heat dissolution curve. Integration of this curve gave the value of dissolution enthalpy.

Preprints (www.preprints.org) | NOT PEER-REVIEWED | Posted: 4 October 2021 doi:10.20944/preprints202110.0053.v1

3. Results

Figure2 shows XRD pattern of synthesized Li_3N (a) and Fe_2N (b) powders. All peaks are in good correlation with database one. Li_3N has *P6/mmm* space group with lattice parameters a=3.6711 Å, b=3.6711 Å and c=3.8770 Å, which are in good correlation with [12] and PDF #30-0759. Fe_2N reflection peaks also are in good correlation with [13] and PDF #50-0978. Space group of Fe_2N is *P312* with lattice parameters a=4.7912 Å, b=4.7912 Å and c=4.416 Å.

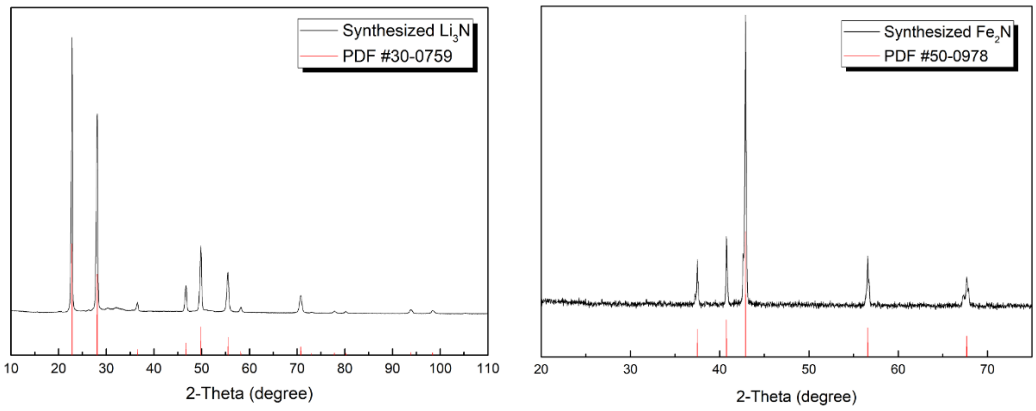

(**a**) (**b**)

Figure 2. XRD pattern of synthesized (a) Li3N at 170°C for 5 h at N2 atmosphere (709 kPa) and (b) Fe2N at 530°C for 5 h at NH3 atmosphere.

Figure 3 shows XRD-pattern of Li_3N, Fe_2N and Li_3FeN_2 after heat treatment at Netzsch APTAK chamber, tube furnace with ammonia atmosphere and tube furnace with nitrogen atmosphere, respectively. Parameters *a* and *c* calculated by the Rietveld method for Li_3FeN_2 are a=4.872 Å, b=9.677 Å and c=4.792 Å, respectively, *Ibam* space group. XRD patterns of Li_3FeN_2 synthesized at different temperatures are shown on Figure 3. Sample synthesized at 850ºC shows high purity of 97.2 % with Li_2O impurity. Other samples include such impurities as Li_2O (PDF #01-076-9237), Li_5FeO_4 (PDF #01-075-1253), $LiFeO_2$ (PDF #74-2284) and $Li_2O_{0.75}N_{0.25}$ (PDF #01-080-4542).

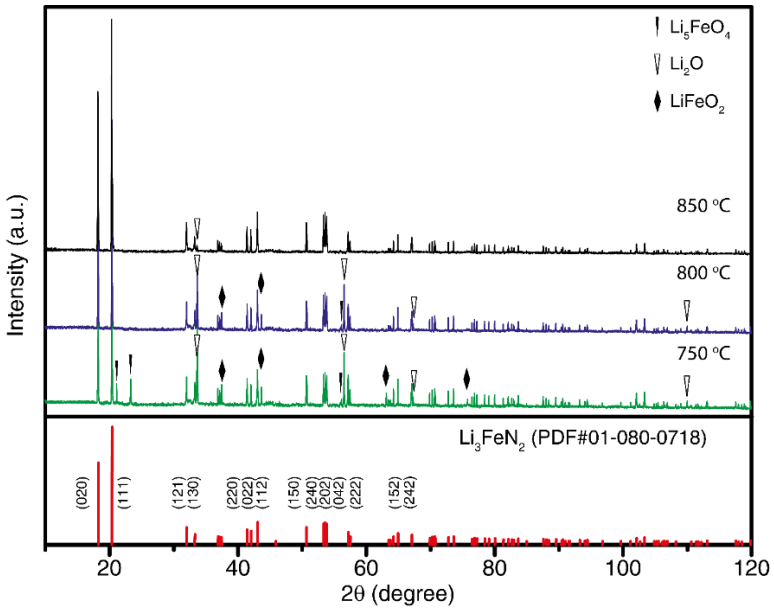

Figure 3. XRD patterns of Li_3FeN_2 after heat treatment at 750, 800 and 850 °C for 10 h at N2 atmosphere. The vertical lines in the bottom indicate diffraction positions of Li3FeN2 structure (PDF #01-080-0718).

Preprints (www.preprints.org) | NOT PEER-REVIEWED | Posted: 4 October 2021 doi:10.20944/preprints202110.0053.v1

Electrochemical performance of lithium-ion cell is shown on Figure 4. Charge and discharge capacity at beginning of life (BOL) is about 371 mAh g^{-1} and 343 mAh g^{-1}, after 100 cycles are 357 $mAhg^{-1}$ and 329 mAh g^{-1}, respectively, are shown on Figure 4, a. Coulombic efficiency is 92.7% and 89.5% before cycling (BOL) and after 100 cycles.

The structure refinement defined that Li^{+} is in *4b* and *8g*, Fe^{+3} is in *4a* and N^{-3} is in *8j* sites. All calculations were carried out with using TOPAS 4 software by Bruker. The final structure parameters (including site occupancy) are listed in Table 2.

Table 2. Structure characteristics of Li3FeN2.

Atom/void	Site	g	x	y	z
Li1	8g	0.91	0.0	0.25745	0.25
Li2	4b	1	0.0	0.5	0.25
Fe	4a	1	0.0	0.0	0.25
N	8j	0.98	0.219979	0.113757	0.5

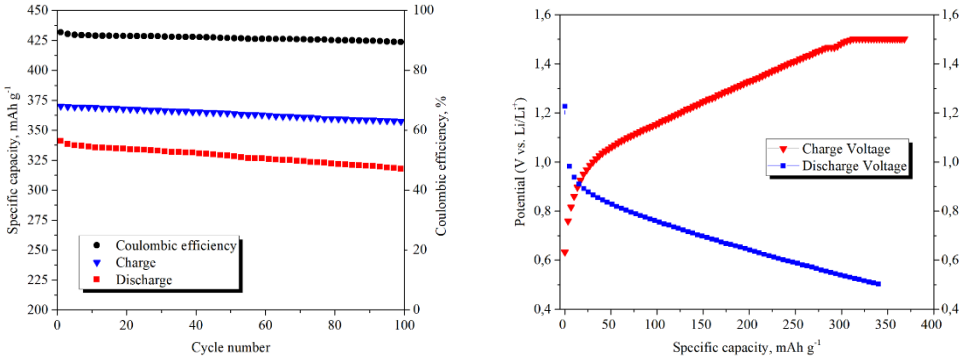

(**a**) (**b**)

Figure 4. Cycling performance (a) and charge-discharge curve at constant current 0.1 C (b).

Theoretical capacity of Li_3FeN_2 with whole lithium deintercalation using Faraday's law is

$$C_T = z \cdot F/M \quad (1)$$

where *z* is lithium ions of compound stoichiometry, C_T is theoretical capacity in $mAh \cdot g^{-1}$, *F* is Faraday constant and *M* is molar mass of Li_3FeN_2 compound. Theoretical capacity is equal to C_T = 768 mAh g^{-1} by formula (1). Discharge capacity is 343 $mAh \cdot g^{-1}$, that is about 44.7% of theoretic capacity (C_T).

4. Discussion

4.1. The standard enthalpy of formation

The enthalpy of Li_3FeN_2 (LFN) formation from single nitrides is calculated according the following equation ($\Delta_{ox}H_{LFN}$):

$$Li_3N + 0.5Fe_2N + 0.25N_2 \rightarrow Li_3FeN_2, \quad (2)$$

and single nitrides were synthesized by reactions, described in Experimental section:

$$6Li + N_2 \rightarrow 2Li_3N, \quad (3)$$

$$2Fe + 2NH_3 \rightarrow 2Fe_2N + 3H_2, \quad (4)$$

Preprints (www.preprints.org) | NOT PEER-REVIEWED | Posted: 4 October 2021 doi:10.20944/preprints202110.0053.v1

For enthalpy calculation we used thermodynamic cycle with the following reactions, Figure 5:

$$Li_3FeN_2 + 6HCl_{(aq)} \rightarrow 3LiCl_{(aq)} + FeCl_{3(aq)} + N_2\uparrow + 3H_2, \quad (5)$$

$$Li_3N + 4HCl_{(aq)} \rightarrow 3LiCl + NH_4Cl, \quad (6)$$

$$2Fe_2N + 8HCl_{(aq)} \rightarrow 4FeCl_2 + 2NH_3 + H_2, \quad (7)$$

$$N_2 + 8HCl_{(aq)} \rightarrow 2NH_4Cl + 3Cl_2, \quad (8)$$

where the subscript *(aq)* means "aqueous". The standard enthalpy of this reaction ($\Delta_d H_{LFN}$) has been measured directly in the calorimeter. The value obtained from calorimetry was equal to −1972.96 ± 25 J g^{-1}, Table 3.

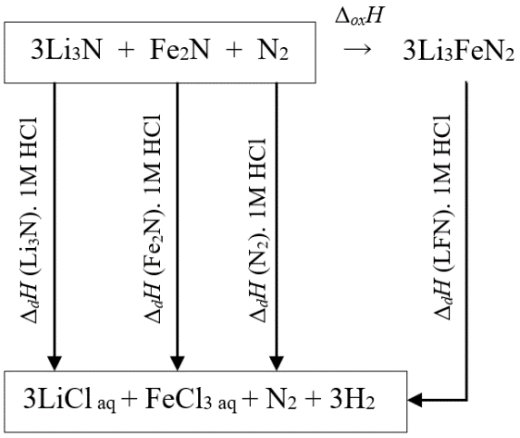

Figure 5. Thermochemical cycle scheme. Dissolution enthalpy connection of Li3FeN2 with its formation enthalpies from single nitrides.

The resulting value of $\Delta_{ox}H_{LFN}$ is obtained by next equation:

$$\Delta_{ox}H_{LFN} = \Delta_d H_{Li3N} + 0.5\Delta_d H_{Fe2N} + 0.25\Delta_d H_{N2} - \Delta_d H_{LFN} \quad (9)$$

The values of $\Delta_d H_{Li3N}$, $\Delta_d H_{Fe2N}$ and $\Delta_d H_{N2}$ were also measured by calorimetry method. Measurement results are shown at Table 3. The value of $\Delta_{ox}H_{LFN}$ by formula (9) is equal to -94.833 kJ mol^{-1}. This value is negative, it means that Li_3FeN_2 is a stable phase and there is an energy benefit in the formation of Li_3FeN_2 from single nitrides.

Table 3. Values of specific and molar enthalpies of dissolution in 1 mol dm^{-3} aqueous HCl at 298 K, p = 101 kPa.

Compound	Specific enthalpy, J g^{-1}	Molar mass, g mol^{-1}	Molar enthalpy of dissolution, kJ mol^{-1}	Ref.
Li_3N	- 3 163,853 ± 30	34,83	-110,197 ± 1,7	this work
Fe_2N	- 13,79 ± 1,5	125,701	-1,734 ±0,04	this work
N_2	- 71,716 ± 10	28,014	-2,56 ± 0,12	this work
Li_3FeN_2	- 1 972,96 ± 25	104,684	-206,537 ± 2,8	this work
$Li_3Na_3N_2$	- 2 285,96 ± 13,4	117,807	-269,3018	[9]

Finally, it is possible now to calculate the enthalpy of Li_3FeN_2 formation from elements by formula:

$$\Delta_f H_{LFN} = \Delta_f H_{Li3N} + 0.5\Delta_f H_{Fe2N} + 0.25\Delta_f H_{N2} + \Delta_{ox} H_{LFN}. \quad (10)$$

Standard enthalpies for the calculation were taken from the handbooks [14, 15], Table 4.

Preprints (www.preprints.org) | NOT PEER-REVIEWED | Posted: 4 October 2021 doi:10.20944/preprints202110.0053.v1

Table 4. Standard enthalpies of formation from elements ($\Delta_f H^0$)

Compound	$\Delta_f H^\circ_{298.15}$, kJ mol^{-1}	Reference
$Li_3N_{(cryst)}$	-196.78 ± 0.3	[14]
$Fe_2N_{(cryst)}$	-3.77 ± 0.1	[14]
$N_{2(gas)}$	8.67 ± 0.1	[15]
$Li_3FeN_{2(cryst)}$	-291.331 ± 5.7	this work
$LiCaN_{(cryst)}$	-216.8 ± 10.8	[16]
$Li_3BN_{2(cryst)}$	-534.5 ± 16.7	[17]
$Li_3AlN_{2(cryst)}$	-567.8 ± 12.4	[17]
$LiMoN_{2(cryst)}$	-386.0 ± 6.4	[18]
Li_7MnN_4	-661	[19]

The subscripts (cryst) and (gas) mean "crystalline" and "gaseous", correspondingly.

The calculated value of the enthalpy of Li_3FeN_2 formation by formula (10) is -291.331 ± 5.7 kJ mol^{-1}, Table 4. Enthalpy of formation $\Delta_f H^0$ for Li_3FeN_2 has the same order as those for similar compounds, namely lithium metallonitrides (Table 4), that confirms correctness of the measurements. This value can be recommended to use in thermodynamic estimation and simulations of Li_3FeN_2 reactivity.

4.2. The isobaric heat capacity

The temperature dependence of the isobaric heat capacity of the Li_3FeN_2 is shown on Figure6. According to XRD data (Figure 3), obtained powder material contains a certain amount of lithium oxide Li_2O. This amount must be taken in account for calculating the heat capacity of the Li_3FeN_2. This impurity could appear during synthesis process or contact with oxygen in air atmosphere. XRD quantitative methods have limitations, but the heat capacity of a two-phase system must be recalculated by additive consideration:

$$mC_p = m(LFN)C_p(LFN) + m(Li_2O)C_p(Li_2O), \quad (11)$$

where C_p is a cpecific heat capacity at constant pressure and m is a mass. The sample weight consists of synthesized compound (Li_3FeN_2) and impurity (Li_2O). So, the heat capacity of Li_3FeN_2) is expressed from eq. (11) as:

$$C_p(LFN) = \frac{mC_p - m(Li_2O)C_p(Li_2O)}{m(LFN)} \quad (12)$$

The weight of the components can be found from the sample total mass, calculating through the mass fraction of lithium oxide, $\omega(Li_2O)$:

$$m(Li_2O) = m\omega(Li_2O) \quad (13)$$

and

$$m(LFN) = m[1-\omega(Li_2O)] \quad (14)$$

According to eq. (13) and (14), eq. (12) can be written as follows:

$$C_p(LFN) = \frac{C_p - C_p(Li_2O)\omega(Li_2O)}{1 - \omega(Li_2O)} \quad (15)$$

Thereby, the heat capacity of LFN can be calculated from the experimental data and heat capacity of lithium oxide impurity. For eq. (15) it is necessary to know temperature dependence of the lithium oxide specific heat capacity. For this, tabular data for the lithium oxide heat capacity at constant pressure [15] was used. For temperature range (300--900 K) the commonly used polynomial formula for the heat capacity:

$$C_p = a + bT - cT^{-2} \quad (16)$$

where T is absolute temperature; a, b, c – empirical coefficients. The obtained coefficients for lithium oxide are: a = 76,666 J mol^{-1} K^{-1}, b = –13,63·10^{-3} J mol^{-1} K^{-2}, c = –18,624·10^5 J mol^{-1} K. The heat capacity of Li_3FeN_2 for 300-900 K temperature range was recalculated using

Preprints (www.preprints.org) | NOT PEER-REVIEWED | Posted: 4 October 2021 doi:10.20944/preprints202110.0053.v1

eq. (16) and (15) considering Li_2O impurity presence. According to XRD data (Figure 3) Li_3FeN_2 contains about 2.8±0.04 wt% Li_2O. Experimental and recalculated LFN heat capacity is shown on Figure6 and Table 5. Empirical values for heat capacity were calculated by Neumann-Kopp rule. This rule prescribes to calculate the molar heat capacity of complex compound from the heat capacities of constituent elements by adding them in corresponding with compound stoichiometry. But this calculation method gives good results for room temperatures and rough results for high temperatures. For more accurate results binary compounds were used instead to single elements (especially if all the components are in the same aggregate state):

$$C_p(CN) = \sum n(BN)C_p(BN) \quad (17)$$

where C_p is molar heat capacity at constant pressure, n is a stoichiometric coefficient, *CN* and *BN* are complex and binary nitride, correspondingly. For LFN, eq. (17) can be written as (according to eq. (2)):

$$C_p\ (LFN) = C_p\ (Li_3N) + 0.5C_p\ (Fe_2N) + 0.25C_p\ (N_2) \quad (18)$$

The temperature dependence of the heat capacity calculated from eq. (18) using tabular data [15] is also shown on Figure 6 and Table 5.

Table 5. The temperature dependence of experimental (exp.), recalculated by eq. (15) (rec.) and calculated by Neumann-Kopp (N-K) rule (eq. 18) heat capacities (Cp) of Li3FeN2(s).

T, K	C_p(exp.), J K^{-1} mol^{-1}	C_p(rec.), J K^{-1} mol^{-1}	C_p(N-K), J K^{-1} mol^{-1}
300	126,9	124,1	117,8
400	134,1	132,6	130,7
500	146,3	144,3	141,9
600	160,5	158,3	152,8
700	173,8	171,9	163,4
800	183,3	180,7	173,6
900	186,1	178,8	183,5

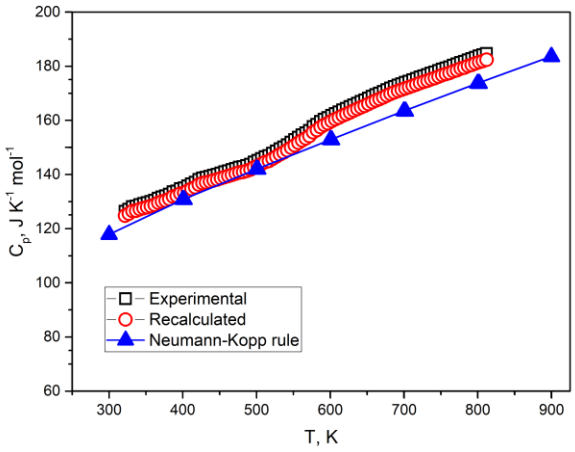

Figure 6. Temperature dependences of the experimental, recalculated and Neumann-Kopp rule heat capacities of Li_3FeN_2. The line for Neuman-Kopp rule is given as an approximating allometric line.

The temperature dependence of the heat capacity determined from eq. (18) using tabular data [20] is shown on Figure 6 and Table 5. The temperature dependence of the heat capacity calculated by Neumann-Kopp rule is in good correlation with recalculated heat capacity (taking into account Li_2O impurity amount). However, XRD quantitative analysis gives rough results for small presence of compounds in material. For another quantitative methods the amount of impurities can be measured more accurately, for example thermogravimetry or volumetric methods.

Preprints (www.preprints.org) | NOT PEER-REVIEWED | Posted: 4 October 2021 doi:10.20944/preprints202110.0053.v1

4.3. Entropy

Entropy is another thermodynamic function that should be calculated. Planck's postulate says that the entropy of an ideal crystal at 0 K is equal to zero. So, the absolute value of the entropy can be calculated from the formula:

$$S(T) = \int_0^{T_1} \frac{C_p(T)}{T} dT + \frac{\Delta H_1}{T_1} + \int_{T_1}^{T_2} \frac{C_p(T)}{T} dT + \frac{\Delta H_2}{T_2} + \cdots + \int_{T_k}^{T} \frac{C_p(T)}{T} dT \quad (19)$$

where S is entropy, ΔH_k is enthalpy of the k-th phase transition, T_k is temperature of the k-th phase transition ($0 < T_k < T$). Since the entropy can be calculated by Neumann-Kopp rule and if there are no phase transition till calculation temperature, entropy can be also calculated by Neumann-Kopp rule:

$$S(T) = \int_0^{T} \frac{\sum C_p(T, BN)}{T} dT = \sum \int_0^{T} \frac{C_p(T, BN)}{T} dT = \sum S(T, BN), \quad (20)$$

where BN is the binary nitride compound (see eq. (17)). According to eq. (17) and (18), eq. (20) can be written in the following way:

$$S\ (LFN) = S(Li_3N) + 0.5S(Fe_2N) \quad (21)$$

The entropy of Li_3FeN_2 at room temperature is 113.2 J mol^{-1} K^{-1} according to eq. (21) and tabular data [15, 20]. Additive rule for entropy calculation is suitable if the sum of the molar volumes of binary compounds differs a bit with the molar volume of the complex compound [21]. Thus, the molar volume for Li_3N is 27.2 cm^3 mol^{-1} (ϱ=1.28 g cm^{-3} [21]), for Fe_2N is 19.8 cm^3 mol^{-1} (ϱ=6.35 g cm^{-3} [21]) and for Li_3FeN_2 is 33.9 cm^3 mol^{-1} (ϱ=3.09 g cm^{-3} [22]). The sum of the molar volumes of binary nitrides with their corresponding coefficients is 37.1 cm^3 mol^{-1} and differs about 9% of the LFN molar volume, which allows usage of additive scheme.

Also, the LFN entropy can be calculated by W.Herz rule [23]:

$$S^0_{298} = K_H (M/C_{p,298})^{1/3} m, \quad (22)$$

where K_H is Herz constant (K_H =20.5), M is molar mass, $C_{p,298}$ is isobaric heat capacity, m is atoms per formula. According to eq. (22) and considering $C_{p,298}$ from Table 5 the LFN entropy is 116.2 J mol^{-1} K^{-1}. Thus, the LFN entropy calculated by Herz rule is in good correlation with Neumann-Kopp rule result.

4.4. The standard Gibbs free energy

The enthalpy of formation and entropy calculated above makes possible to calculate the standard Gibbs free energy of Li_3FeN_2 formation at room temperature:

$$\Delta_f G^0_{298} = \Delta_f H^0_{298} - 298\Delta_f S^0_{298}, \quad (23)$$

The resulting value of the Gibbs free energy for Li_3FeN_2 at room temperature is -276,7 kJ mol^{-1}.

The next reaction is suggested for determination of stability against metallic lithium with subsequent calculation of the Gibbs free energy at room temperature:

$$3Li + Li_3FeN_2 = 2Li_3N + Fe \quad (24)$$

To determine the Gibbs free energy of reaction it is required to subtract from $\Delta_f G^0_{298}$ of the reaction products values of the Gibbs energy for initial reagents. The $\Delta_f G^0_{298}$ for single elements is equal to zero, for Li_3N and is -128.6 kJ mol^{-1} [20]. The Li_3FeN_2 Gibbs free energy has been determined above. Thus, the Gibbs free energy for reaction (24) is 19.5 kJ mol^{-1} and this reaction is thermodynamically impossible. Finally, Li_3FeN_2 is stable against metallic lithium at room temperature.

5. Conclusions

The thermodynamic characteristics were determined for Li_3FeN_2 anode material for lithium-ion battery. Two-step synthesis method allowed to produce highly pure compound with less than 3%wt. of Li_2O impurity according to XRD data. The enthalpy of Li_3FeN_2 formation from binary nitrides was calculated according to the measured enthalpy of dissolution of reagents and product of Li_3FeN_2 formation reaction. The obtained value is equal to -206,5 ± 2,8 kJ mol^{-1}. The Li_3FeN_2 standard enthalpy of formation from elements is equal -291.3 ± 5.7 kJ mol^{-1}. This value can be used in further thermodynamic modeling and determinations.

The heat capacity value was recalculated taking into account presence of Li_2O impurity. The temperature dependence of the heat capacity is in good correlation with calculated by Neumann-Kopp rule. Finaly, the heat capacity can be described by formula $C_p(T) = 78{,}997+0{,}132 \times T + 4.654 \cdot 10^5 \times T^{-2}$, where T is absolute temperature. The LFN entropy is equal to 113.2 J mol^{-1} K^{-1}, the Gibbs free energy of Li_3FeN_2 formation is -276,7 kJ mol^{-1}. Calculations confirm that Li_3FeN_2 material is stable against metallic lithium. All thermodynamic values and functions can be used for modelling and further calculations.

Author Contributions: Conceptualization, A.P. and P.N.; methodology, D.A.; software, P.K.; validation, D.A., K.P. and Q.W.; formal analysis, A.P.; investigation, D.A. and K.P.; resources, Q.W.; data curation, P.N.; writing—original draft preparation, D.A.; writing—review and editing, P.N.; visualization, K.P.; supervision, A.P.; project administration, Q.W.; funding acquisition, Q.W. All authors have read and agreed to the published version of the manuscript.

Funding: The research is partially funded by the Ministry of Science and Higher Education of the Russian Federation: Advanced Digital Technologies (contract No. 075-15-2020-934 dated from 17.11.2020)

Institutional Review Board Statement: Not applicable.

Informed Consent Statement: Not applicable.

Data Availability Statement: The data presented in this study are available on request from the corresponding author.

Conflicts of Interest: The authors declare no conflict of interest.

References

1. Bruce, P. G., Scrosati, B., & Tarascon, J. M. Nanomaterials for rechargeable lithium batteries. *Angewandte Chemie International Edition*, **2008**, *47*(16), 2930-2946.
2. Popovich, A. A., Maximov, M. Y., Nazarov, D. V., Novikov, P. A., Silin, A. O., & Shamshurin, A. I. Low-temperature deposition of tin (IV) oxide films for thin-film power sources. *Russian Journal of Applied Chemistry*, **2016**, *89*(5), 805-808.
3. Nazarov, D. V., Maximov, M. Y., Novikov, P. A., Popovich, A. A., Silin, A. O., Smirnov, V. M., ... & Rumyantsev, A. M. Atomic layer deposition of tin oxide using tetraethyltin to produce high-capacity Li-ion batteries. *Journal of Vacuum Science & Technology A: Vacuum, Surfaces, and Films*, **2017**, *35*(1), 01B137.
4. Balakrishnan, P. G., Ramesh, R., & Kumar, T. P. Safety mechanisms in lithium-ion batteries. *Journal of power sources*, **2006**, *155*(2), 401-414.
5. Aravindan, V., Lee, Y. S., & Madhavi, S. Research progress on negative electrodes for practical Li-ion batteries: beyond carbonaceous anodes. *Advanced Energy Materials*, **2015**, *5*(13), 1402225.
6. Nitta, N., Wu, F., Lee, J. T., & Yushin, G. Li-ion battery materials: present and future. *Materials today*, **2015**, *18*(5), 252-264.
7. Schön, J. C., Wevers, M. A. C., & Jansen, M. Investigation of the possible ternary nitrides in the system Li3N/Na3N. *Solid state sciences*, **2000**, *2*(4), 449-456.
8. Somer, M., Carrillo-Cabrera, W., Peters, E. M., Peters, K., & Von Schnering, H. G. Crystal structure of lithium beryllium nitride, LiBeN. *Zeitschrift für Kristallographie-Crystalline Materials*, **1996**, *211*(9), 635-635.
9. Yamane, H., Okabe, T. H., Ishiyama, O., Waseda, Y., & Shimada, M. Ternary nitrides prepared in the Li3N–Mg3N2 system at 900–1000 K. *Journal of alloys and compounds*, **2001**, *319*(1-2), 124-130.
10. Frankenburger, W., Andrussow, L., & Dürr, F. Eine neue Komplexverbindung von Lithium, Eisen und Stickstoff. Ein Beitrag zur Frage der Stickstoffbindung an Eisen. *Zeitschrift für Elektrochemie und angewandte physikalische Chemie*, **1928**, *34*(9), 632-637.
11. Fromont, M. PREPARATION AND STUDY OF DOUBLE NITRIDE LI3FEN2. *Revue de Chimie Minerale*, **1967**, *4*(2), 447.
12. Cabana, J., Ling, C. D., Oró-Solé, J., Gautier, D., Tobias, G., Adams, S., ... & Palacin, M. R. Antifluorite-type lithium chromium oxide nitrides: synthesis, structure, order, and electrochemical properties. *Inorganic chemistry*, **2004**, *43*(22), 7050-7060.
13. Lei, X., Wang, J., Peng, R., & Wang, W. The controllable magnetic properties of Fe3N nanoparticles synthesized by a simple urea route. *Materials Research Bulletin*, **2020**, *122*, 110662.

14. Veryatin U.d., Mashirev V.P., Ryabtsev N. G., Tarasov V. I., Rogozkin B. D., Korobov I. V. Thermodinamicheskie Svoitsva Neorganicheskikh Veshchestv; Atomizdat: Moscow, Russia, 1965.
15. Glushko V.P., Gurvich L.V., Bergman G.A., Veits I.V., Medvedev V.A., Khachkuruzov G.A., Yungman V.S. Thermodinamicheskie Svoitsva Individual'nykh Veshchestv; Nauka: Moscow, Russia, 1978.
16. McHale, J. M., Navrotsky, A., Kowach, G. R., Balbarin, V. E., & DiSalvo, F. J. Energetics of Ternary Nitrides: Li− Ca− Zn− N and Ca− Ta− N Systems. *Chemistry of materials*, **1997**, *9*(7), 1538-1546.
17. McHale, J. M., Navrotsky, A., & DiSalvo, F. J. Energetics of Ternary Nitride Formation in the (Li, Ca)−(B, Al)− N System. *Chemistry of materials*, **1999**, *11*(4), 1148-1152.
18. Elder, S. H., DiSalvo, F. J., Topor, L., & Navrotsky, A. Thermodynamics of ternary nitride formation by ammonolysis: application to lithium molybdenum nitride (LiMoN2), sodium tungsten nitride (Na3WN3), and sodium tungsten oxide nitride (Na3WO3N). *Chemistry of materials*, **1993**, *5*(10), 1545-1553.
19. He, G., Herbst, J. F., Ramesh, T. N., Pinkerton, F. E., Meyer, M. S., & Nazar, L. Investigation of hydrogen absorption in Li 7 VN 4 and Li 7 MnN 4. *Physical Chemistry Chemical Physics*, **2011**, *13*(19), 8889-8893.
20. Pankratz, L. B. Thermodynamic properties of carbides, nitrides, and other selected substances, **1995**.
21. Knunyants, I. L. Khimicheskaya entsiklopediya; Sovetskaya entsiklopediya: Moscow, Russia, 1988.
22. Gudat, A., Kniep, R., Rabenau, A., Bronger, W., & Ruschewitz, U. Li3FeN2, a ternary nitride with 1∞[FeN423−] chains: Crystal structure and magnetic properties. *Journal of the Less Common Metals*, **1990**, *161*(1), 31-36.
23. Morachevskiy A. G., Sladkov I. B., Firsova Ye. G. Termodinamicheskiye raschety v khimii i metallurgii; Lan': St.Petersburg, Russia, 2018.